Calculation of thermal pressure coefficient of dense fluids using the linear isotherm regularity

Vahid Moeini[1,3]**, Feridon Ashrafi**[2]**, Mahnaz Karri**[2] **and Hojatolaeh Rahimi**[1]

[1] Payame Noor University, Behshahr Center, Behshahr, Iran
[2] Payame Noor University, Sari Center, Sari, Iran

E-mail: V_moeini@yahoo.com

Abstract
New parameters of the linear isotherm regularity, the so-called LIR equation of state, are used to calculate the thermal pressure coefficient of dense fluids. The extent of the deviation between real thermal pressure coefficients and thermal pressure coefficients by applying LIR are best expressed through the use of new parameters in LIR. In this paper, the temperature dependence of LIR parameters in the form of a first order have been developed to second order and third order, and the temperature derivatives of new parameters are used to calculate thermal pressure coefficients. The resulting model accurately predicts thermal pressure coefficients from the lower density limit at the Boyle density and from the triple temperature up to about double the Boyle temperature. The upper density limit appears to be reached at 1.4 times the Boyle density. These problems have led us to try to establish a function for accurate calculation of the thermal pressure coefficients, based on LIR theory for different fluids.

1. Introduction

One of the most difficult problems in the context of the thermodynamics lies in the shortage of experimental data for some basic quantities such as thermal pressure coefficients (TPC), which are tabulated for extremely narrow temperature ranges, normally around the ambient temperature for several types of liquids. Furthermore, measurements of the thermal pressure coefficients made by different researchers often reveal systematic differences between their estimates.

The idea has been presented of a simple method using direct calculation of the thermal pressure coefficient in place of using the equation of state to analyze the experimental p–v–T data. The equation of state described in papers is explicit in the Helmholtz energy A, with the two independent variables of density ρ and temperature T. At a given temperature, the thermal pressure coefficient can be determined from the Helmholtz energy [1].

Other work has led us to try to establish a correlation function for accurate calculation of the thermal pressure

coefficient for different fluids over wide temperature and pressure ranges [2]. The most straightforward way of deriving the thermal pressure coefficient is to calculate the thermal pressure coefficient with the use of the principle of corresponding states, which covers wide temperature and pressure ranges. The principle of corresponding states calls for the reduced thermal pressure at a given reduced temperature and density to be the same for all fluids. This is true, since the corresponding states approach is appropriate for conditions of low density, in which the fluid molecules are far apart and thus have little interaction. Moreover, at low density, the gas behaves ideally and its thermal pressure coefficient is temperature independent and approaches ρR in the zero-density limit. However, as the density increases, molecular interactions become increasingly important and the principle of corresponding states fails. The leading term of this correlation function is the thermal pressure coefficient of a perfect gas, which each gas obeys in the low-density range. Using this condition, the thermal pressure coefficient of different supercritical fluids and refrigerants can be predicted up to densities of $\rho \approx \rho_C$. As mentioned before, as the density increases, molecular interactions become increasingly

---

[3] Author to whom any correspondence should be addressed.

important and the principle of corresponding states fails [3]. It found out 'empirically' that at high densities it is possible to apply the principle of corresponding states to different fluids according to the magnitude of their critical densities versus $\rho_C = 10 \ \text{mol dm}^{-3}$.

A general regularity was reported for pure dense fluids, namely testing literature results for p–v–T for pure dense fluids, according to which $(Z - 1)V^2$ is linear with respect to ρ^2 for each isotherm, where $Z \equiv pv/RT$ is the compression factor [4]. This equation of state works very well for all types of dense fluids, for densities greater than the Boyle density but for temperatures below twice the Boyle temperature. The regularity was originally suggested on the basis of a simple lattice-type model applied to a Lennard-Jones (12, 6) fluid. We shall refer to this equation of state as the 'linear isotherm regularity', or simply LIR from now on. The LIR is used to investigate some empirically known regularities [5, 6].

In the present work, LIR has been used to calculate the thermal pressure coefficient. The purpose of this paper is to point out an expression for the thermal pressure coefficient of dense fluids using LIR. In this paper, in section 1, we present a simple method that keeps the first-order temperature dependence of parameters in LIR versus inverse temperature. Then, the thermal pressure coefficient is calculated from LIR. In section 2, the temperature dependence of the parameters in LIR has been developed to second order. In section 3, the temperature dependence of parameters in LIR has been developed to third order and then the thermal pressure coefficient is calculated by LIR in each state.

2. Theory

Liquids and dense fluids are usually considered to be complicated on a molecular scale; they show a number of simple regularities [7]. The first is the Tait–Murnaghan relation, in which the bulk modulus (reciprocal compressibility) of a liquid (or solid) is linear in pressure [8]. The second is the linear relation between the temperature and density at unit compression factor [9], which was discovered empirically in 1906. The third is the common bulk modulus point, in which all liquid isotherms of the reduced bulk modulus as a function of molar volume intersect at essentially a single point [10]. The fourth is the linear isotherm for dense fluids [3], for which we attempt to calculate the internal pressure by modeling the average configurational potential energy and then take its derivative with respect to volume. This assumes that any kinetic energy contribution to the internal energy will vanish on taking the derivative, since the temperature is held constant. It also approximates the average potential energy by summing the contribution from nearest neighbors only, and assuming that the average number of nearest neighbors is proportional to the density, as is the case for liquid argon, rubidium, and cesium [11]. Combining the foregoing results, a general regularity that was reported for pure dense fluids, according to which $(Z - 1)V^2$ is linear with respect to ρ^2, each isotherm is,

$$(Z - 1) V^2 = A + B\rho^2, \tag{1}$$

where $Z \equiv pv/RT$ is the compression factor, $\rho = 1/V$ is the molar density, and A and B are the temperature-dependent parameters [3]. It is shown that this regularity is compatible with equations of state based on statistical–mechanical theory [12]. The model thus not only mimics the linearity of $(Z - 1)V^2$ versus ρ^2 but also predicts the temperature dependence intercept and slope. This result immediately shows why A has much similarity to the second virial coefficient. It has the same temperature dependence as that of a van der Waals gas, which usually gives a fair representation of the temperature dependence for real gases in the vicinity of the Boyle temperature [3]. The compression factor of the system can be given by using the LIR:

$$\frac{p}{\rho RT} = 1 + A\rho^2 + B\rho^4. \tag{2}$$

Therefore, the compression factor $Z \equiv pv/RT$ versus ρ^2 becomes quadratic for each isotherm. Using the experimental data, the temperature dependence of the parameters will be tested in the following sections.

2.1. First-order temperature dependence of parameters

We first derive the pressure by applying LIR, and then use the first-order temperature dependence of the parameters to get the final thermal pressure coefficient for the dense fluid, where

$$A = A_2 - \frac{A_1}{RT} \tag{3}$$

$$B = \frac{B_1}{RT}. \tag{4}$$

Here A_1 and B_1 are related to the intermolecular attractive and repulsive forces, respectively, while A_2 is related to the non-ideal thermal pressure and RT has its usual meaning.

In the present work, the starting point in the derivation is equation (2). By substitution of equations (3) and (4) in equation (2), the pressure can be given by using the LIR:

$$p = \rho RT + A_2\rho^3 RT - A_1\rho^3 + B_1\rho^5. \tag{5}$$

We first derive an expression for the thermal pressure coefficient using the first-order temperature dependence of the parameters. The final result is $\text{TPC}_{\text{LIR}}^{(1)}$:

$$\left(\frac{\partial p}{\partial T}\right)_\rho = R\rho + A_2 R\rho^3. \tag{6}$$

According to equation (6), the experimental value of density and the value of A_2 by applying LIR can be used to calculate the value of the thermal pressure coefficient. According to the LIR, A is linear versus $1/T$; the intercept gives the value of A_2. The values of A_2 for nine fluids (Ar, N_2, CO, CH_4, C_2H_6, n-C_4H_{10}, iso-C_4H_{10}, C_6H_6 and C_6H_5–CH_3) are listed in table 1, together with the temperature range of the experimental data and the coefficient of determination. We begin with C_6H_6 in its liquid range for calculating the thermal pressure coefficient. Figure 1 shows the experimental values of the thermal pressure coefficient versus density for C_6H_6
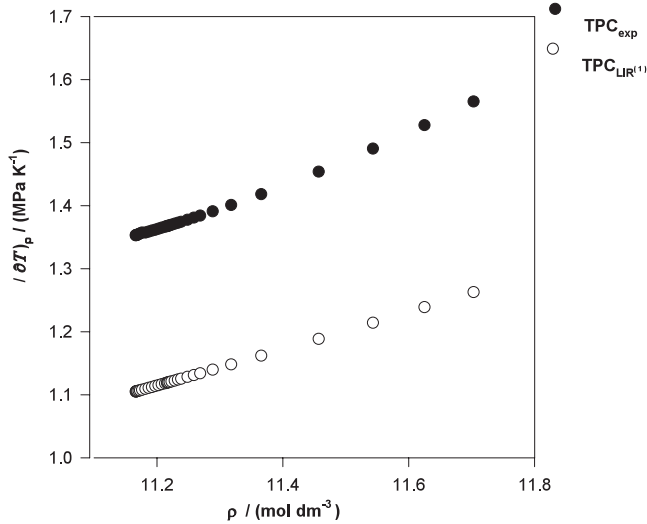
Figure 1. The experimental values of the thermal pressure coefficient [15] versus density for C_6H_6 fluid are compared with the thermal pressure coefficient using the LIR$^{(1)}$ at 300 K.

Table 1. The calculated values of A_2 for different fluids using equation (3) and the coefficient of determination (R^2).

Fluid	A_2	$T_{min}-T_{max}$ (K)	R^2
Ar [a]	0.6547	84–400	0.9986
N_2 [b]	0.6333	100–600	0.9976
CO [c]	0.7795	70–210	0.9997
CH_4 [d]	0.7455	100–400	0.9927
C_2H_6 [d]	1.4550	150–285	0.9960
n-C_4H_{10} [d]	1.6582	160–500	0.9919
Iso-C_4H_{10} [d]	1.7191	200–380	0.9967
C_6H_6 [e]	1.3327	280–700	0.9962
C_6H_5–CH_3 [f]	3.3818	180–680	0.9718

[a] Reference [13].
[b] Reference [14].
[c] Reference [15].
[d] Reference [16].
[e] Reference [17].
[f] Reference [18].

fluid compared with the thermal pressure coefficient using the LIR$^{(1)}$ at 300 K. The thermal pressure coefficient using the LIR$^{(1)}$ model yields inaccurate results for the liquid phase. Also, this deviation is significant for the supercritical phase. Also, we predict that this deviation leads to inaccurate values of A_2; for this purpose, we plot A versus $1/T$. Figures 2(a), (b) and 3(a), (b) show plots of A and B versus inverse temperature for benzene [17] and toluene [18], respectively. It is clear that A and B versus inverse temperature are not first order.

2.2. Second-order temperature dependence of parameters

In order to solve this problem, the LIR equation of state in the form of truncated temperature series of A and B parameters has been developed to second order for dense fluids. Figures 4(a) and (b) show plots of A and B parameters versus inverse temperature for toluene fluid. It is clear that A and B versus inverse temperature are second order. Thus, extending
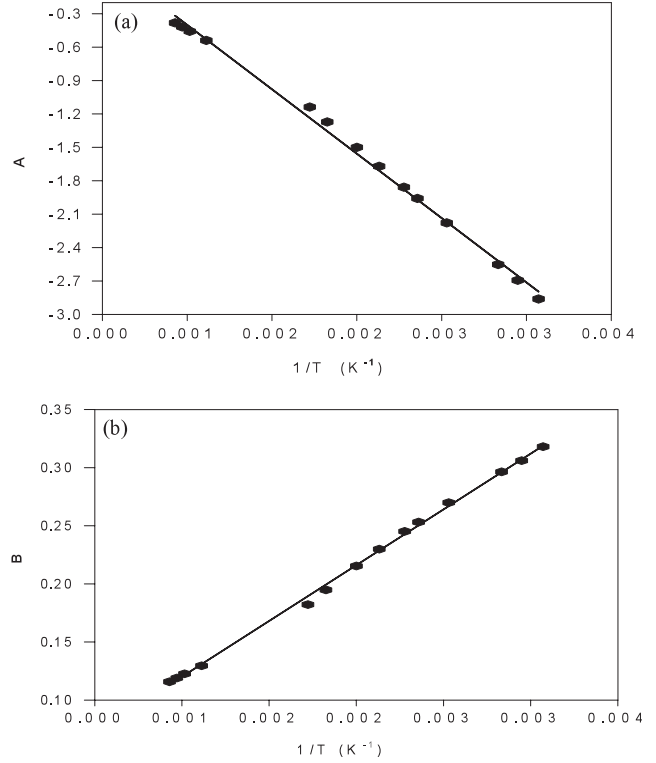

Figure 2. (a) Plot of A versus inverse temperature. The solid line is the linear fit to the A data points, for C_6H_6. (b) Plot of B versus inverse temperature. The solid line is the linear fit, for C_6H_6.

parameters A and B, we obtain the second-order equation as

$$A = A_1 + \frac{A_2}{T} + \frac{A_3}{T^2} \tag{7}$$

$$B = B_1 + \frac{B_2}{T} + \frac{B_3}{T^2}. \tag{8}$$

The starting point in the derivation is equation (2) again. By substitution of equations (7) and (8) into equation (2), we obtain the pressure for a dense fluid:

$$p = \rho RT + A_1\rho^3 RT + A_2\rho^3 R + \frac{A_3\rho^3 R}{T}$$
$$+ B_1\rho^5 RT + B_2\rho^5 R + \frac{B_3\rho^5 R}{T}. \tag{9}$$

The A and B parameters and their temperature derivatives were calculated from this model, and the final result is, for thermal pressure coefficient to form TPC$_{LIR}^{(2)}$,

$$\left(\frac{\partial p}{\partial T}\right)_\rho = \rho R + A_1\rho^3 R - \frac{A_3\rho^3 R}{T^2} + B_1\rho^5 R - \frac{B_3\rho^5 R}{T^2}. \tag{10}$$

Therefore, it is possible to calculate the thermal pressure coefficient at each density and temperature by knowing A_1, A_3, B_1 and B_3. For this purpose we have plotted extended parameters of A and B versus $1/T$ that intercept, and the coefficients show the values of A_1, A_3, B_1 and B_3 that are given in table 2. For comparison, figure 5 shows the experimental values of the thermal pressure coefficient versus density for C_6H_6 fluid, which are compared with the thermal pressure coefficient using LIR$^{(1)}$ and LIR$^{(2)}$ at 300 K.

Table 2. The calculated values of A_1 and A_3 using equation (7) and B_1 and B_3 using equation (8) for different fluids, and the coefficient of determination (R^2).

Fluid	A_1	A_3	R^2	B_1	B_3	R^2
Ar	0.4991	$-3\,706.358\,7$	0.9995	-6.8495	-47.0034	0.9988
N_2	0.5643	$-2\,842.113\,6$	0.9994	-0.0170	-413.7710	0.9997
CO	0.7401	$-541.531\,6$	0.9997	-0.01536	-238.4968	0.9996
CH_4	0.4379	$-9\,763.747\,9$	0.9989	0.0222	840.0285	0.9948
C_2H_6	0.6025	$-35\,228.587\,9$	0.9964	-0.0157	$2\,175.0593$	0.9964
n-C_4H_{10}	1.0532	$-38\,685.930\,6$	0.9946	-0.0273	$1\,795.5946$	0.9843
Iso-C_4H_{10}	0.8837	$-61\,899.017\,01$	0.9992	-0.0657	$1\,393.3018$	0.9974
C_6H_6	0.7560	$-106\,881.225\,0$	0.9994	-0.01602	$1\,482.2852$	0.9984
C_6H_5–CH_3	0.4660	$-324\,389.763\,1$	0.9999	0.04642	24\,435.4658	0.9997

Figure 3. (a) Plot of A versus inverse temperature. The solid line is the linear fit to the A data points, for $C_6H_5CH_3$. (b) Plot of B versus inverse temperature. The solid line is the linear fit, for $C_6H_5CH_3$.
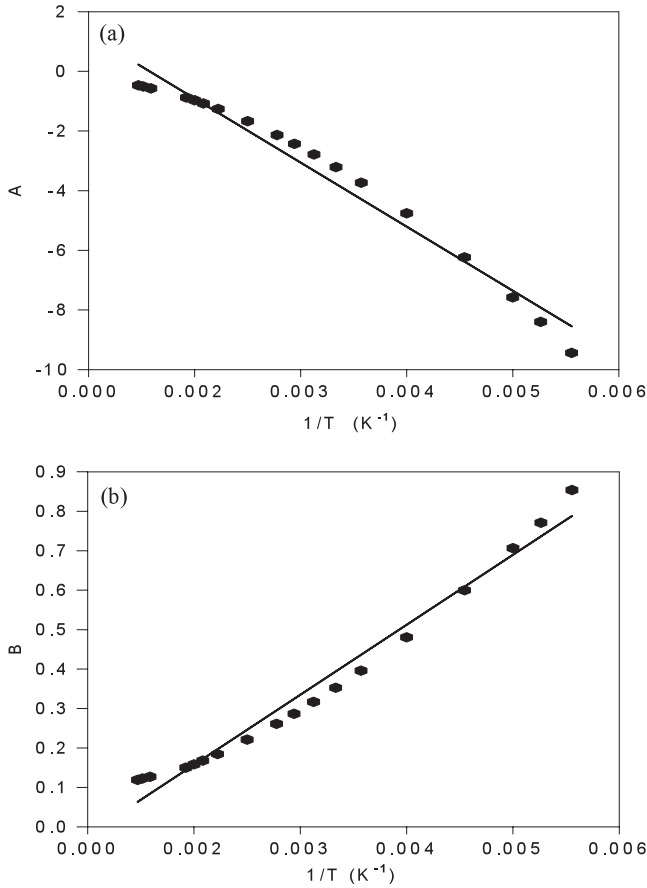

Figure 4. (a) Plot of A versus inverse temperature. The solid line is the linear fit to the A data points, for $C_6H_5CH_3$. (b) Plot of B versus inverse temperature. The solid line is the linear fit, for $C_6H_5CH_3$.
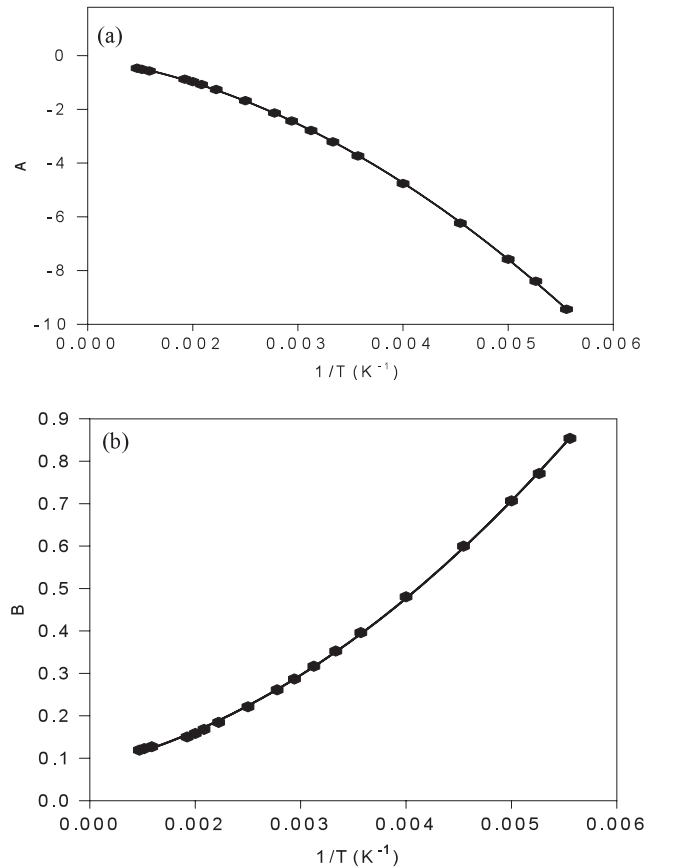
2.3. Third-order temperature dependence of parameters

In another step, we performed a test to form the truncated temperature series of A and B parameters to third order:

$$A = A_1 + \frac{A_2}{T} + \frac{A_3}{T^2} + \frac{A_4}{T^3} \tag{11}$$

$$B = B_1 + \frac{B_2}{T} + \frac{B_3}{T^2} + \frac{B_4}{T^3}. \tag{12}$$

The starting point in the derivation is equation (2) again. By substitution of equations (11) and (12) into equation (2), we

obtain the pressure for a dense fluid:

$$p = \rho RT + A_1\rho^3 RT + A_2\rho^3 R + \frac{A_3\rho^3 R}{T} + \frac{A_4\rho^3 R}{T^2}$$
$$+ B_1\rho^5 RT + B_2\rho^5 R + \frac{B_3\rho^5 R}{T} + \frac{B_4\rho^5 R}{T^2}. \tag{13}$$

The final result is for the thermal pressure coefficient to form $\text{TPC}_{\text{LIR}}^{(3)}$:

$$\left(\frac{\partial p}{\partial T}\right)_\rho = \rho R + A_1\rho^3 R - \frac{A_3\rho^3 R}{T^2} - \frac{2A_4\rho^3 R}{T^3} + B_1\rho^5 R$$
$$- \frac{B_3\rho^5 R}{T^2} - \frac{2B_4\rho^5 R}{T^3}. \tag{14}$$

Table 3. The calculated values of A_1, A_3 and A_4 using equation (11) and B_1, B_3 and B_4 using equation (12) for different fluids, and the coefficient of determination (R^2).

Fluid	A_1	A_3	A_4	R^2	B_1	B_3	B_4	R^2
Ar	0.5573	1 588.2075	−255 206.700 9	0.9995	−0.0185	−1 674.3079	78 438.7202	0.9993
N_2	0.5067	−11 194.1323	480 305.114 4	0.9997	−0.0165	−328.2972	−4 915.3978	0.9997
CO	0.3769	−15 207.4785	510 407.750 11	0.9999	0.0216	1260.1355	−52 155.7557	0.9999
CH_4	0.6916	15 246.1106	−1 303 481.829 8	0.9994	−0.0346	−4761.6612	291 952.9006	0.9975
C_2H_6	−3.6242	−596 340.0834	37 599 682.264 2	0.9999	0.7107	98 611.1758	−6 462 115.5835	0.9995
n-C_4H_{10}	−1.2557	−563 655.4140	43 116 619.415 2	0.9994	0.2815	72 010.114 61	−5 766 835.6597	0.9968
Iso-C_4H_{10}	−0.7316	−434 114.1607	32 935 125.996 0	0.9994	0.10589	40 931.1604	−3 498 472.2574	0.9976
C_6H_6	−0.5826	−858 368.2127	99 883 029.983 8	0.9998	0.1615	101 177.5628	−13 250 883.3324	0.9996
C_6H_5–CH_3	−0.16701	−431 729.1284	10 471 322.000 3	0.9999	0.1049	44 466.7211	−1 954 117.4199	0.9998

Figure 5. Experimental values of the thermal pressure coefficient versus density for C_6H_6 fluid are compared with the thermal pressure coefficient using LIR$^{(1)}$ and LIR$^{(2)}$ at 300 K.
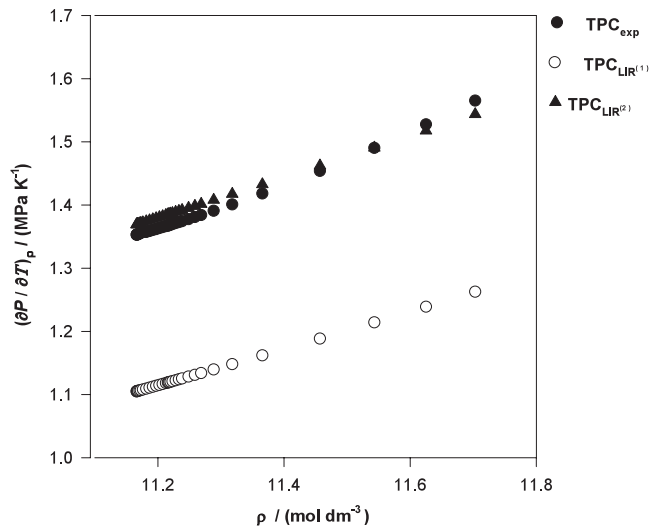

Figure 6. Experimental values of the thermal pressure coefficient versus density for C_6H_6 fluid compared with the thermal pressure coefficient using LIR$^{(1)}$, LIR$^{(2)}$ and LIR$^{(3)}$ at 300 K.

On the basis of equation (14), to obtain the thermal pressure coefficient it is necessary to determine the values of A_1, A_3, A_4, B_1, B_3 and B_4; these values are given in table 3. In contrast, figures 6 and 7 show the experimental values of the thermal pressure coefficient versus density for benzene as a liquid and as a supercritical fluid, which are compared with the thermal pressure coefficient using LIR$^{(1)}$, LIR$^{(2)}$ and LIR$^{(3)}$ at 300 and 680 K, respectively.

3. Experimental tests and discussion

The thermal pressure coefficient is computed for dense liquid and supercritical fluids using three different models. To investigate the first-order temperature dependence of the parameter A, the nine fluids serve as our primary test, because of the abundance of available p–v–T data. The A_2 values calculated via equation (2) have been evaluated by applying the coefficient of determination. The results are summarized in table 1. In examining the ability of the LIR theory to calculate the thermal pressure coefficients of dense fluids, benzene [17] and toluene [18] serve because of the abundance of available thermal pressure coefficients data. Such data are more limited for the other fluids examined. When we
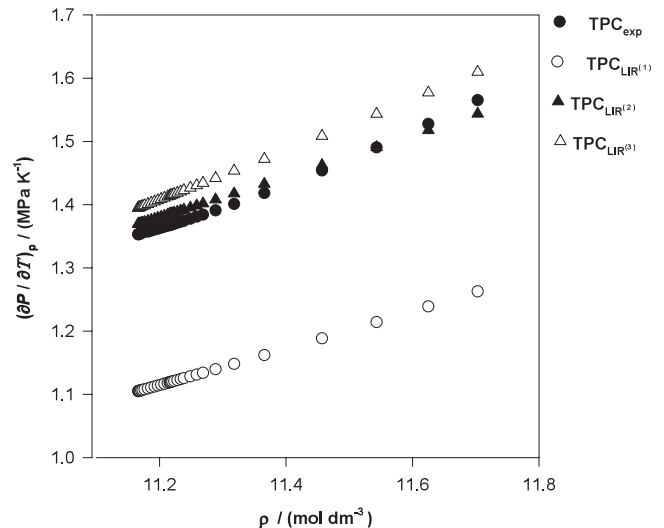

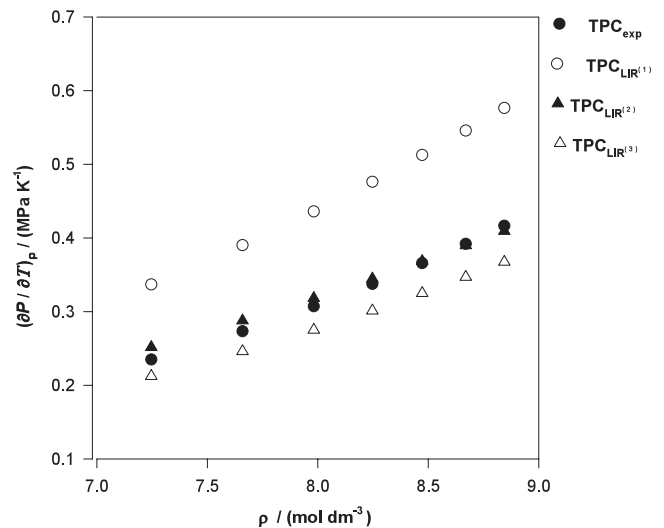**Figure 7.** Experimental values of the thermal pressure coefficient versus density for C_6H_6 fluid compared with the thermal pressure coefficient using LIR$^{(1)}$, LIR$^{(2)}$ and LIR$^{(3)}$ at 680 K.

restricted the temperature series of the parameters A and B to first order, it was seen that the points from the low densities for TPC$_{LIR}^{(1)}$ deviate significantly from the experimental data.

Table 4. Comparison between the calculated and experimental values of $(\partial P/\partial T)\rho$ for liquid C_6H_6.

T (K)	P (MPa)	ρ (mol l^{-1})	$(\partial p/\partial T)_\rho$ (MPa K^{-1})			
			Exp	LIR$^{(1)}$	LIR$^{(2)}$	LIR$^{(3)}$
300.0000	0.0500	11.1661	1.3530	1.1051	1.3691	1.3949
300.0000	0.1013	11.1666	1.3532	1.1053	1.3693	1.3951
300.0000	0.1500	11.1671	1.3533	1.1054	1.3695	1.3953
300.0000	0.2000	11.1677	1.3534	1.1056	1.3696	1.3955
300.0000	0.3000	11.1687	1.3537	1.1059	1.3700	1.3959
300.0000	0.5000	11.1709	1.3549	1.1065	1.3706	1.3967
300.0000	0.7000	11.1730	1.3558	1.1071	1.3713	1.3975
300.0000	1.0000	11.1762	1.3573	1.1080	1.3723	1.3988
300.0000	1.5000	11.1815	1.3573	1.1094	1.3740	1.4008
300.0000	2.0000	11.1867	1.3589	1.1109	1.3756	1.4028
300.0000	2.5000	11.1920	1.3604	1.1124	1.3773	1.4048
300.0000	3.0000	11.1972	1.3619	1.1139	1.3789	1.4068
300.0000	3.5000	11.2024	1.3635	1.1153	1.3806	1.4088
300.0000	4.0000	11.2076	1.3650	1.1168	1.3822	1.4107
300.0000	4.5000	11.2128	1.3666	1.1183	1.3839	1.4127
300.0000	4.8000	11.2159	1.3675	1.1191	1.3849	1.4139
300.0000	4.8757	11.2167	1.3677	1.1194	1.3851	1.4142
300.0000	5.0000	11.2180	1.3681	1.1197	1.3855	1.4147
300.0000	5.2000	11.2200	1.3688	1.1203	1.3862	1.4155
300.0000	5.5000	11.2231	1.3697	1.1212	1.3871	1.4167
300.0000	6.0000	11.2282	1.3713	1.1226	1.3888	1.4186
300.0000	6.5000	11.2334	1.3729	1.1241	1.3904	1.4206
300.0000	7.0000	11.2384	1.3745	1.1255	1.3920	1.4226
300.0000	8.0000	11.2486	1.3777	1.1284	1.3952	1.4265
300.0000	9.0000	11.2587	1.3810	1.1313	1.3984	1.4304
300.0000	10.0000	11.2687	1.3842	1.1341	1.4016	1.4342
300.0000	12.0000	11.2885	1.3909	1.1398	1.4080	1.4419
300.0000	15.0000	11.3179	1.4010	1.1482	1.4174	1.4534
300.0000	20.0000	11.3656	1.4183	1.1620	1.4327	1.4721
300.0000	30.0000	11.4569	1.4539	1.1887	1.4623	1.5085
300.0000	40.0000	11.5432	1.4905	1.2143	1.4906	1.5434
300.0000	50.0000	11.6251	1.5277	1.2390	1.5177	1.5772
300.0000	60.0000	11.7031	1.5652	1.2628	1.5437	1.6098

Table 5. Comparison between the calculated and experimental values of $(\partial P/\partial T)\rho$ for supercritical C_6H_6.

T (K)	P (MPa)	ρ (mol l^{-1})	$(\partial p/\partial T)_\rho$ (MPa K^{-1})			
			Exp	LIR$^{(1)}$	LIR$^{(2)}$	LIR$^{(3)}$
680.0000	40.0000	7.2468	0.2351	0.3369	0.2518	0.2125
680.0000	50.0000	7.6593	0.2735	0.3903	0.2879	0.2461
680.0000	60.0000	7.9817	0.3073	0.4360	0.3183	0.2753
680.0000	70.0000	8.2470	0.3377	0.4763	0.3448	0.3013
680.0000	80.0000	8.4728	0.3658	0.5127	0.3685	0.3251
680.0000	90.0000	8.6697	0.3920	0.5458	0.3898	0.3470
680.0000	100.0000	8.8443	0.41660	0.5765	0.4094	0.3675

Table 6. Comparison between the calculated and experimental values of of $(\partial P/\partial T)\rho$ for liquid C_6H_5–CH_3.

T (K)	P (MPa)	ρ (mol l^{-1})	$(\partial p/\partial T)_\rho$ (MPa K^{-1})			
			Exp	LIR$^{(1)}$	LIR$^{(2)}$	LIR$^{(3)}$
280.0000	0.0100	9.5255	1.3821	2.5240	1.4252	1.3733
280.0000	0.0200	9.5256	1.3821	2.5241	1.4252	1.3733
280.0000	0.0500	9.5258	1.3821	2.5243	1.4252	1.3733
280.0000	0.1013	9.5262	1.3821	2.5246	1.4252	1.3733
280.0000	0.1500	9.5265	1.3821	2.5248	1.4253	1.3733
280.0000	0.3000	9.5275	1.3820	2.5256	1.4253	1.3733
280.0000	0.5000	9.5289	1.3820	2.5267	1.4254	1.3733
280.0000	0.7000	9.5303	1.3819	2.5278	1.4255	1.3734
280.0000	1.0000	9.5323	1.3819	2.5293	1.4256	1.3734
280.0000	1.5000	9.5357	1.3818	2.5320	1.4258	1.3735
280.0000	2.0000	9.5391	1.3818	2.5346	1.4260	1.3735
280.0000	2.5000	9.5425	1.3818	2.5373	1.4262	1.3736
280.0000	3.0000	9.5459	1.3818	2.5399	1.4265	1.3736
280.0000	3.5000	9.5493	1.3818	2.5426	1.4267	1.3737
280.0000	4.0000	9.5527	1.3819	2.5453	1.4269	1.3738
280.0000	4.2365	9.5542	1.3819	2.5464	1.4269	1.3738
280.0000	4.5000	9.5560	1.3820	2.5478	1.4270	1.3738
280.0000	5.0000	9.5594	1.3821	2.5505	1.4272	1.3739
280.0000	5.5000	9.5627	1.3822	2.5531	1.4274	1.3739
280.0000	6.0000	9.5660	1.3824	2.5557	1.4276	1.3739
280.0000	6.5000	9.5694	1.3826	2.5583	1.4278	1.3740
280.0000	7.0000	9.5727	1.3827	2.5609	1.4280	1.3740
280.0000	8.0000	9.5793	1.3832	2.5661	1.4283	1.3741
280.0000	9.0000	9.5859	1.3837	2.5713	1.4287	1.3741
280.0000	10.0000	9.5924	1.3843	2.5765	1.4290	1.3742
280.0000	12.0000	9.6054	1.3856	2.5867	1.4297	1.3743
280.0000	15.0000	9.6246	1.3879	2.6019	1.4306	1.3743
280.0000	20.0000	9.6550	1.3926	2.6262	1.4318	1.3742
280.0000	25.0000	9.6866	1.3979	2.6515	1.4330	1.3739
280.0000	30.0000	9.7164	1.4037	2.6756	1.4339	1.3734
280.0000	35.0000	9.7455	1.4098	2.6992	1.4346	1.3727
280.0000	40.0000	9.7739	1.4160	2.7224	1.4351	1.3718
280.0000	50.0000	9.8287	1.4285	2.7675	1.4356	1.3696
280.0000	60.0000	9.8811	1.4409	2.8111	1.4355	1.3669
280.0000	70.0000	9.9314	1.4525	2.8535	1.4348	1.3636
280.0000	80.0000	9.9796	1.4633	2.8944	1.4336	1.3598
280.0000	90.0000	10.0260	1.4729	2.9342	1.4320	1.3556
280.0000	100.0000	10.0708	1.4813	2.9729	1.4299	1.3511

derivatives. So, the thermal pressure coefficient gives the form of $TPC_{LIR}^{(2)}$.

We also considered an even more accurate estimate, namely extension of the temperature series of the parameters A and B to third order. Then we introduce the explicit parameters and temperature dependences resulting from the p–v–T data. The final result is for thermal pressure coefficient to form $TPC_{LIR}^{(3)}$. In contrast, figures 8 and 9 show the experimental values of the thermal pressure coefficient versus density for liquid and supercritical fluid toluene, compared with the thermal pressure coefficient using LIR$^{(1)}$, LIR$^{(2)}$ and LIR$^{(3)}$ at 280 and 680 K, respectively. The experimental and calculated values of the thermal pressure coefficient using LIR$^{(1)}$, LIR$^{(2)}$ and LIR$^{(3)}$ are also compared in tables 4–7 for benzene and toluene fluids. Although all three models capture the qualitative features for dense fluids, only the calculated values of the thermal pressure coefficient using the LIR$^{(2)}$ model produce quantitative agreement. Tables 4–7 present a greater test of these models, because only the

To decrease adequately the deviation in the thermal pressure coefficient from the experimental data, it was necessary to extend the temperature series of the parameters A and B to second order. Nevertheless, it is only for some monatomic fluid similar to Ar that the temperature dependences of the parameters A and B themselves are satisfactory to first order. Therefore, the present approach for obtaining the thermal pressure coefficient from p–v–T data contrasts with the experimental data by extension of the temperature series of the parameters A and B to second order and its
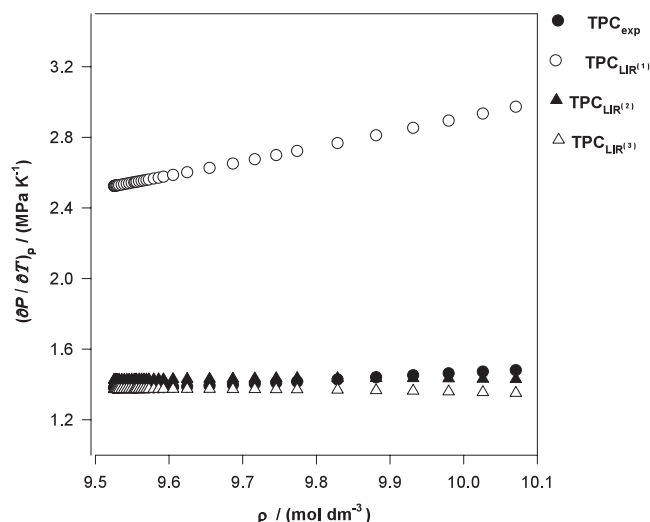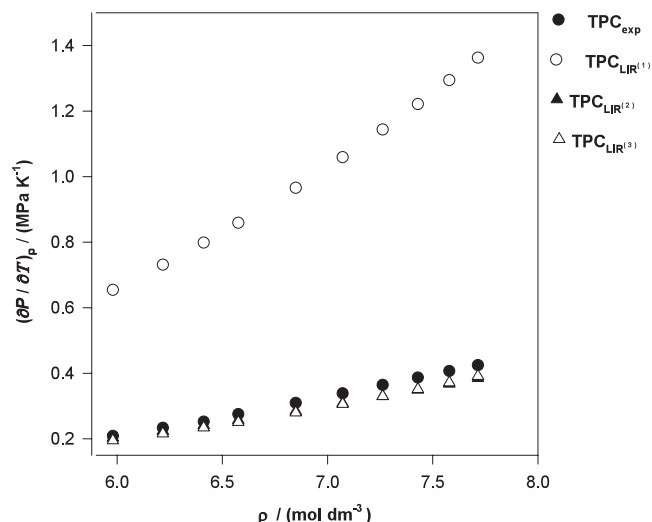
Figure 8. Experimental values of the thermal pressure coefficient versus density for $C_6H_5CH_3$ fluid compared with the thermal pressure coefficient using $LIR^{(1)}$, $LIR^{(2)}$ and $LIR^{(3)}$ at 280 K.

Table 7. Comparison between the calculated and experimental values of $(\partial P/\partial T)_\rho$ for supercritical C_6H_5–CH_3.

T (K)	P (MPa)	ρ (mol l^{-1})	$(\partial p/\partial T)_\rho$ (MPa K^{-1})			
			Exp	$LIR^{(1)}$	$LIR^{(2)}$	$LIR^{(3)}$
660.0000	25.0000	5.9795	0.2088	0.6544	0.2031	0.1949
660.0000	30.0000	6.2172	0.2337	0.7314	0.2236	0.2159
660.0000	35.0000	6.4112	0.2526	0.7987	0.2413	0.2342
660.0000	40.0000	6.5762	0.2753	0.8591	0.2570	0.2508
660.0000	50.0000	6.8491	0.3096	0.9657	0.2846	0.2801
660.0000	60.0000	7.0721	0.3390	1.0593	0.3085	0.3060
660.0000	70.0000	7.2623	0.3645	1.1438	0.3299	0.3296
660.0000	80.0000	7.4293	0.3870	1.2216	0.3495	0.3513
660.0000	90.0000	7.5788	0.4070	1.2943	0.3677	0.3718
660.0000	100.0000	7.7149	0.4247	1.3630	0.3847	0.3912

$LIR^{(2)}$ model is able to predict accurately both the thermal pressure coefficient of the liquid and supercritical fluids. The $LIR^{(3)}$ model yields good results for toluene, but deviates significantly for benzene, in contrast to the experimental values of the thermal pressure coefficient, whereas the $LIR^{(1)}$ model is rather inaccurate for both benzene and toluene fluids.

4. Result

In this paper, we have derived an expression for the thermal pressure coefficient of dense fluids (N_2, Ar, CO, CH_4, C_2H_6, n-C_4H_{10}, iso-C_4H_{10}, C_6H_6 C_6H_5–CH_3) using the linear isotherm regularity. Unlike previous models, it has been shown in this work that the thermal pressure coefficient can be obtained without employing any reduced Helmholtz energy. Only p–v–T experimental data have been used for calculating the thermal pressure coefficient [19]. Comparison of the calculated values of the thermal pressure coefficient using the linear isotherm regularity with the values obtained experimentally show that validity of the use of the

Figure 9. Experimental values of the thermal pressure coefficient versus density for $C_6H_5CH_3$ fluid compared with the thermal pressure coefficient using $LIR^{(1)}$, $LIR^{(2)}$ and $LIR^{(3)}$ at 660 K.

linear isotherm regularity for studying the thermal pressure coefficient of monatomic dense fluids is doubtful. The validity of the use of the linear isotherm regularity equation state for calculating the thermal pressure coefficient of polyatomic dense fluids is also imprecise. In this work, it has been shown that the temperature dependences of the intercept and the slope using the linear isotherm regularity are nonlinear. This problem has led us to try to obtain the expression for the thermal pressure coefficient using the extended intercept and slope of the linearity parameters versus inverse temperature to second order. The thermal pressure coefficients predicted from this simple model are in good agreement with experimental data. The results show that the accuracy of this method is generally quite good.

Acknowledgment

References

[1] Moeini V 2006 *J. Phys. Chem.* B **110** 3271
[2] Ghayeb Y, Najafi B, Moeini V and Parsafar G A 2003/2004 *High Temp.–High Pressures* **35/36** 217
[3] Parsafar G and Mason E A 1994 *Phys. Rev.* B **49** 3049
[4] Parsafar G and Mason E A 1993 *J. Phys. Chem.* **97** 9048
[5] Parsafar G, Moeini V and Najafi B 2001 *Iran J. Chem. Chem. Eng.* **20** 37
[6] Najafi B, Parsafar G and Alavi S 1995 *J. Phys. Chem.* **99** 9248
[7] Barker J A and Henderson D 1976 *Rev. Mod. Phys.* **48** 316
[8] Macdonald J R 1969 *Rev. Mod. Phys.* **40** 316
[9] Xu J and Herschbach D R 1992 *J. Phys. Chem.* **96** 2307
[10] Huang Y H and O' Connell J P 1987 *Fluid Phase Equilib.* **37** 75
[11] Hensel F and Uchtmann H 1989 *Annu. Rev. Phys. Chem.* **40** 61
[12] Ihm G, Song Y and Mason E A 1991 *J. Chem. Phys.* **94** 3839

[13] Stewart R B and Jacobsen T 1989 *J. Phys. Chem. Ref. Data* **18** 639

[14] Jacobsen R T, Stewart R B and Jahangiri M 1986 *J. Phys. Chem. Ref. Data* **15** 735

[15] Goodwin R D 1985 *J. Phys. Chem. Ref. Data* **14** 849

[16] Younglove B A and Ely J F 1987 *J. Phys. Chem. Ref. Data* **16** 577

[17] Goodwin R D 1988 *J. Phys. Chem. Ref. Data* **17** 1541

[18] Goodwin R D 1989 *J. Phys. Chem. Ref. Data* **18** 1565

[19] Ely J F and McQuarrie D A 1974 *J. Chem. Phys.* **60** 4105